ATLAS NOTE

ATLAS-CONF-2011-046

March 22, 2011

ATLAS Muon Momentum Resolution in the First Pass Reconstruction of the 2010 *p-p* Collision Data at $\sqrt{s} = 7$ TeV

The ATLAS Collaboration

Abstract

A measurement of the muon momentum resolution is presented for the first pass reconstruction of ATLAS *p-p* collision data in 2010, which uses preliminary calibration and alignment constants. The measurement is based on a sample of 40 pb^{-1} of LHC *p-p* collision data at $\sqrt{s} = 7$ TeV collected with muon triggers. The momentum resolution is extracted from the width of the di-muon mass distribution in $Z \to \mu\mu$ decays and the comparison of the independent measurements of muons from $Z \to \mu\mu$ and $W \to \mu\nu_\mu$ decays provided by the two ATLAS tracking systems, the Inner Detector and Muon Spectrometer. This note documents the status of the muon system performance used in 2010 physics analyses.

1 Introduction

The physics programme of the ATLAS experiment [1] at the LHC includes investigations of many processes with final state muons. The ATLAS detector is equipped with a Muon Spectrometer (MS) optimized to provide a momentum measurement with a relative resolution designed to be better than 3% over a wide p_{T} range and 10% at $p_{\mathrm{T}} = 1$ TeV, where p_{T} is the muon momentum component in the plane transverse to the beam axis. The momentum in the MS is measured from the deflection of the muon trajectory in the magnetic field generated by a system of air-core toroid coils. The MS track is reconstructed using three layers of precision drift tube (MDT) chambers in the pseudorapidity[1] range $|\eta| < 2.0$ and two layers of MDT chambers behind one layer of cathode strip chambers (CSC) for $2.0 \leq |\eta| < 2.7$. Large and small MDT and CSC chambers alternate to cover the full angle in the transverse plane, ϕ, following the azimuthal segmentation of the toroid magnet system. Three layers of resistive plate chambers (RPC) in the barrel region ($|\eta| < 1.05$) and three layers of thin gap chambers (TGC) in the end-caps ($1.0 < |\eta| < 2.4$) provide fast response to select events with muons in the final state *in real-time*, forming the ATLAS level-1 muon trigger. The trigger chambers also measure the muon trajectory in the non-bending (longitudinal) plane of the spectrometer magnets.

An additional determination of the muon momentum is provided by the Inner Detector (ID) for $|\eta| < 2.5$. The ID is composed of three detectors providing coordinate measurements for track reconstruction inside a solenoidal magnetic field of 2 T. A silicon pixel detector is mounted close to the interaction point and is surrounded by a silicon strip detector (SCT). The outermost part is a transition radiation straw tube tracker (TRT) whose full coverage is given up to $|\eta| = 1.9$ in pseudorapidity. Muons entering this analysis are reconstructed as *combined muons*. The underlying muon identification is described in [2] and relies on the principle that first separate tracks are measured in ID and MS before the two tracks are reconstructed as a single trajectory with higher momentum resolution than each of the individual tracks could achieve.

This note documents the muon momentum resolution in the first pass reconstruction of *p*-*p* collision data collected in 2010 corresponding to an integrated luminosity of 40 pb^{-1}. The first pass reconstruction uses preliminary calibration and alignment, therefore it is expected that the measured resolution is poorer than its design value estimated from simulation. The momentum resolution is measured from the width of the di-muon invariant mass distribution in $Z \rightarrow \mu\mu$ decays and from comparisons of the individual ID and MS momentum determination for *combined muons* from $W \rightarrow \mu\nu_{\mu}$ decays.

2 Parametrization of the momentum resolution as a function of transverse momentum and pseudorapidity

The relative resolution on the momentum measurement, $\frac{\sigma(p)}{p}$, is dictated by different effects related to the amount of material that the muon traverses, the spatial resolution of the individual track points and the degree of internal alignment of the two subsystems (see also [3, 4]). The ATLAS MS is designed to provide a uniform momentum resolution as a function of the pseudorapidity. For a given value of η, the resolution can be parametrized in the following way as a function of the transverse component p_{T}:

$$\frac{\sigma(p)}{p} = \frac{p_0^{MS}}{p_{\mathrm{T}}} \oplus p_1^{MS} \oplus p_2^{MS} \cdot p_{\mathrm{T}} \tag{1}$$

where p_0^{MS}, p_1^{MS} and p_2^{MS} are coefficients related to the energy loss in the calorimeters material, multiple scattering and intrinsic resolution terms, respectively. For the ID a similar parametrization can be found. In this case the curvature measurement depends on the track length of the muon in the active material,

[1] The pseudorapidity $\eta = -\ln(\tan(\theta/2))$, where θ is the polar angle measured from the beam line.

which is reduced close to the edge of the TRT fiducial volume. This translates into a uniform response in the central part and a rapidly worsening resolution beyond this region. The following approximate parametrization of the resolution[2] is used:

$$\frac{\sigma(p)}{p} = p_1^{ID} \oplus p_2^{ID}\ p_{\mathrm{T}} \tag{2}$$

for fixed η and $|\eta| < 1.9$. For $|\eta| > 1.9$ and using the muon polar angle θ it is

$$\frac{\sigma(p)}{p} = p_1^{ID} \oplus p_2^{ID}\ p_{\mathrm{T}}\ \frac{1}{\tan^2(\theta)} \tag{3}$$

By considering *combined muons* the analysis is limited to the ID geometrical acceptance ($|\eta| < 2.5$ for a precise momentum measurement). Four regions in pseudorapidity are distinguished for which we expect to have different resolutions in the ID and MS:

- *Barrel* – covering $0 < |\eta| < 1.05$,
- *Transition region* – covering $1.05 < |\eta| < 1.7$,
- *End-caps* – covering $1.7 < |\eta| < 2.0$ and
- *CSC/no TRT* – covering $2.0 < |\eta| < 2.5$.

There are four regions each for $\eta > 0$ and $\eta < 0$. All η regions are studied individually with $Z \to \mu\mu$ decays to probe for a possible η asymmetry in the momentum resolution before combining results for positive and negative η. In addition to the η-dependence the muon momentum resolution in the MS varies also with the azimuthal angle ϕ. Given the limited statistics available, this variation is neglected in the present analysis and the resolution is integrated over ϕ.

3 Data and Monte Carlo samples

The results documented in this note are based on an integrated luminosity of 40 pb^{-1}, obtained with stable LHC beams in the period March to October 2010.

Events are selected on-line by the ATLAS muon trigger chain [5]: no p_{T} threshold requirement is applied at level-1 and an inclusive trigger sample is used for these performance studies. Events have been accepted for this analysis if the ID and MS detectors were in optimal data-taking conditions and both magnet systems were on. For the analysis with single muons from W boson decays we also require the calorimeters to be in optimal data-taking conditions: this additional requirement reduces the integrated luminosity to 29 pb^{-1}.

Experimental data are compared to Monte Carlo simulations of signal and background processes. The simulated processes are generated with Pythia [6], passed through the full simulation of the ATLAS detector based on Geant4 [7, 8], the trigger simulation and the same reconstruction chain used for data. For the signal we use samples of W and Z boson decays into muons, without any additional kinematic filters at the generation or simulation stage. The different background sources used are described in Section 5.3. The simulation describes the performance of a perfectly calibrated and aligned ATLAS detector. Studies with cosmic rays [9] showed shortcomings in the simulation of the intrinsic resolution and module misalignment, neither of which are corrected for in the current simulation. Inactive or non-installed detector parts are modeled by masking or omitting the corresponding components, respectively.

The *p-p* collision and simulated datasets were processed offline with a single version of the reconstruction software. In particular, we report results based on the 2010 first pass ATLAS reconstruction which used preliminary calibration and alignment for the ID and MS.

[2] p_1^{ID} and p_2^{ID} are the multiple scattering and intrinsic resolution terms, respectively

4 Event selection

Collision events are selected by requiring at least one reconstructed Primary Vertex (PV) with a position $|z_{\rm PV}| < 150\,$mm relative to the nominal interaction point and at least 3 ID tracks associated with the PV. Each of the 3 tracks should have at least 1 hit in the pixel detector and at least 6 hits in the SCT. Specific additional requirements for each decay channel, both at the muon and event level, are described in the following paragraphs.

4.1 Muon selection

To select collision events with muon final state we require *combined muons* [2] with:

- At least 1 hit in the pixel detector, 6 hits in the SCT and a number of hits in the TRT compatible with its coverage in pseudorapidity,
- Pseudorapidity $|\eta| < 2.5$.

4.2 Selection of $Z \to \mu\mu$ decays

We select $Z \to \mu\mu$ decays by applying the following requirements:

- Exactly two combined muons, with opposite electric charge, each satisfying the requirements discussed in Section 4.1;
- Each of the selected muons should have a transverse momentum $p_{\rm T} > 20\,$GeV and a direction within the same η region, as defined in Section 2.

4.3 Selection of $W \to \mu\nu_\mu$ decays

The sample of $W \to \mu\nu_\mu$ decays was selected with the following requirements, which were optimized for the measurement of the W boson production cross-section from leptonic decays [10]:

- At least one isolated muon with $p_{\rm T} > 10$ GeV; a muon is considered isolated if the sum of the transverse momenta of the (non-muon) tracks in a cone of $\sqrt{\Delta\eta^2+\Delta\phi^2} = 0.4$ around the muon is less than 20% of the muon $p_{\rm T}$;
- A missing transverse energy $E_{\rm T}^{\rm miss}$, measured using both the calorimetric and muon energy measurements, of at least 25 GeV;
- A reconstructed W boson transverse mass

$$M_T(W) = \sqrt{2(p_{\rm T}^{\mu})(E_{\rm T}^{\rm miss})[1-cos(\phi^{\mu}-\phi^{E_{\rm T}^{\rm miss}})]} \tag{4}$$

  larger than 40 GeV.

This selection suppresses the muon background from decays in flight and heavy flavor decays in jets.

5 Combined fit to the muon resolution components and comparison with results from cosmic ray data

The processes $Z \to \mu\mu$ and $W \to \mu\nu_\mu$ are sensitive to the momentum resolution through two quantities:

- the width of the reconstructed di-muon invariant mass peak at the the Z pole, which is a convolution of the natural width of the Z boson and the muon momentum resolution;
- the difference of the independent momentum measurements of the ID and MS for combined muons in selected $W \to \mu\nu_\mu$ events; this difference is sensitive to the quadratic sum of the ID and MS momentum resolutions.

This section discusses first the individual performance of the two quantities and then presents the technique to parameterize both with a single resolution function for each tracking system. This combination of two independent channels also increases the statistical sensitivity of the momentum resolution on the expected p_{T} and η dependence. Once the actual resolution parameters are measured, correction parameters are provided for the simulated muon p_{T} to reproduce the data. Such corrections are needed in order to accurately measure analysis-level quantities based on the muon p_{T}. These include, for example, an event selection acceptance and the muon contribution to the calculation of the event missing transverse energy.

5.1 Di-muon invariant mass distribution at the Z pole

The resolution contribution to the relative invariant mass width is studied as a function of the η region in cases where both muons are reconstructed in that η region (see event selections in Section 4.2). The di-muon invariant mass distributions are obtained separately from MS and ID track parameters and integrated over all muon p_{T} values. They are then fitted using a convolution of the Z lineshape and two Gaussian functions modelling the detector resolution effects. The two Gaussians are centered at 0. While the full fit range is from 60 to 120 GeV, one core Gaussian is constrained to contain 85% of the di-muon pairs. This value corresponds to the fraction of muons contained within the core Gaussian in the simulation, where the fit was applied without constraint. The Z lineshape, including the Z boson natural width, a photon radiation term and the interference term [11], is given by:

$$f(x) = A\left(\frac{1}{x^2}\right) + B\left(\frac{(x^2-\bar{x}^2)}{(x^2-\bar{x}^2)^2+\sigma_x^2\bar{x}^2}\right) + C\left(\frac{x^2}{(x^2-\bar{x}^2)^2+\sigma_x^2\bar{x}^2}\right) \quad , \tag{5}$$

where x indicates the reconstructed di-muon invariant mass $M_{\mu\mu}$. A, B and C as well as σ_x are fixed parameters, determined from the invariant mass of the muon pair at particle level before detector simulation, while $\bar{x}$ is a free parameter in the fit. The fit function is validated by investigating how well it describes the true Z boson lineshape in simulation. It is also verified that, if let free to fluctuate, the estimates for A, B and C are unbiased.

The mass resolution, i.e. $\sigma(M)$ of the core Gaussian in the fit, is shown in Figure 1 as a function of η region for the MS (left) and ID (right). Variations in η of the detector material, magnetic field bending power and detector acceptance create a structure in the simulated mass resolution that is symmetric in η. The data show the same symmetric structure with the exception that the ID momentum resolution shows an absolute asymmetry in the di-muon invariant mass resolution of about 4% in the region $|\eta| > 2.0$ between positive and negative η. This corresponds to about a 60% fractional difference in resolution between the two sides. The effect is due to a different level of ID misalignment on the two sides, already observed in [12] (see e.g. Figure 5b). This issue was solved for the reprocessing of the full 2010 dataset [13].

An overall discrepancy between simulated and measured resolution is observed in all detector regions. It is partly understood as a result of the limited accuracy with which the calibration and alignment constants were known prior to the first pass reconstruction. For the MS also the material distribution and magnetic field description can, if inaccurate, contribute to a larger resolution at low momenta. The agreement between data and Monte Carlo in the $|\eta| < 1.05$ region of both tracking systems is of the

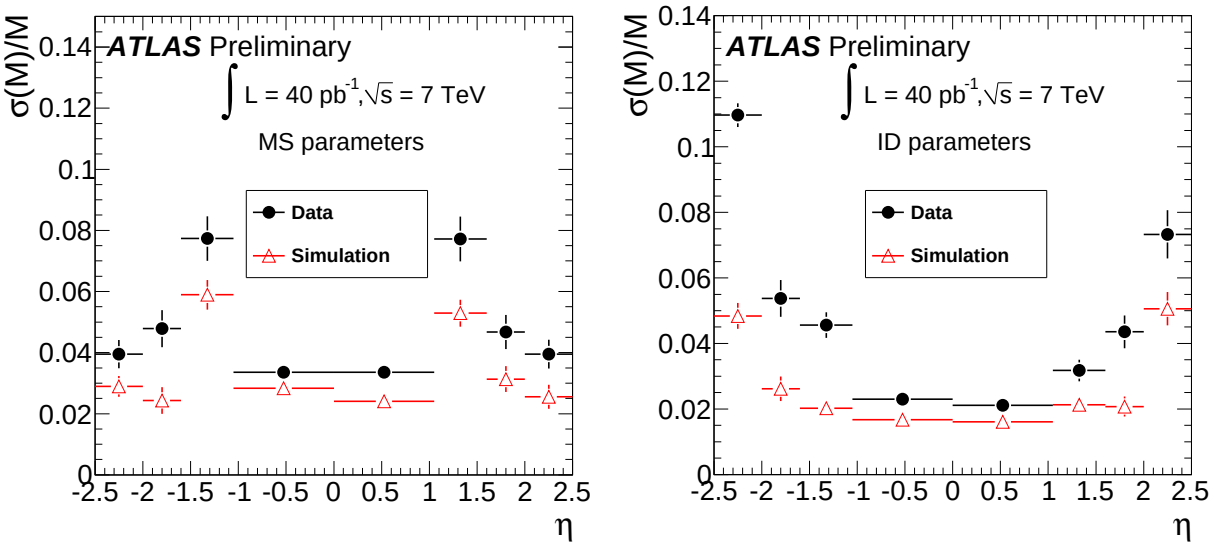

Figure 1: Resolution contribution $\sigma(M)$ to the relative di-muon invariant mass width in data (circles) and simulation (oepn triangles) as a function of η region, for the MS (left) and the ID (right) part of *combined muon* pairs.

same kind as that observed with cosmic ray events [3, 4]. The disagreement for the other regions, which had a smaller exposure to cosmic ray muons, is discussed in detail at the end of Section 5.2.

The value of the fitted invariant mass at the Z pole is sensitive to possible shifts in the momentum scale. The accuracy of the momentum scale is probed by measuring the average deviation of the measured invariant mass from the Z mass world average, which is shown in Figure 2 for combined muons in data and simulation. It is obtained for each of the four $\eta > 0$ and $\eta < 0$ regions and averaged over all muon p_{T} values. A good agreement with the Z mass world average ($M(Z) = 91.1876$ GeV [14]) is observed, except for the two regions within $-2.5 < \eta < -1.7$. There an offset of up to 1.5% is present which is not modelled by simulation. This offset has been further studied by measuring the average deviation separately in the ID and MS. It can be explained by an asymmetry in the magnetic field between the positive and negative end-caps that is taken into account in a more recent version of the track reconstruction code.

5.2 Quadratic sum of the momentum resolution of the Muon Spectrometer and the Inner Detector from $W \to \mu\nu_\mu$ decays

Another way of measuring the muon momentum resolution is to use the redundancy in the ATLAS tracking systems, by comparing the independent momentum measurements for events with single muons. A relative difference in momentum is defined as

$$\rho := \frac{p_{\mathrm{ID}} - p_{\mathrm{MS}}}{p_{\mathrm{ID}}} \quad , \tag{6}$$

where p_{ID} denotes the momentum measurement in the ID and p_{MS} the momentum measured by the MS and extrapolated to the interaction point, taking energy loss into account. As a result the expectation value for ρ is 0 and the width of the distribution is determined by the quadratic sum of the resolutions of the two detectors. Depending on the region of the pseudorapidity and the range of p_{T}, this quantity is dominated by the ID or MS contribution. The use of single muons allows us to probe the quadratic sum of the resolutions of the two detectors as a function of p_{T} from ≈ 20 GeV up to about 120 GeV.

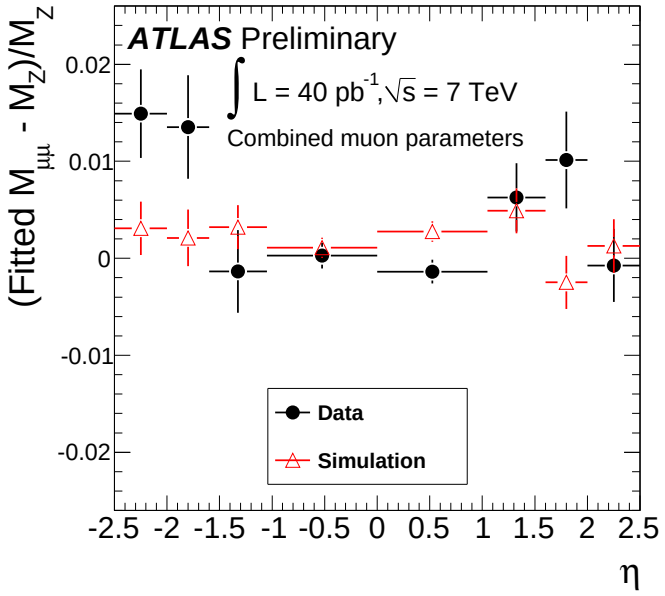

Figure 2: Average deviation of the measured invariant mass from the Z mass world average as function of η region to which the two combined muons are associated. The fitted value corresponds to the $\bar{x}$ in Equation 5. The error bars for both data (circles) and simulation (open triangles) are statistical only.

To extract the resolution as a function of the muon p_{T} and $|\eta|$ the ρ distribution is fitted with a normal distribution, in a range of $\pm$ 1 r.m.s. from the mean of the data distribution. Using about 70 000 selected $W \rightarrow \mu\nu_{\mu}$ decays, the sample is large enough to perform the fitting procedure in six p_{T} bins: 20-25 GeV, 25-35 GeV, 35-45 GeV, 45-55 GeV, 55-70 GeV, >70 GeV. The fitted resolution sum values as a function of p_{T} are shown in Figure 3. Once more the four pseudorapidity regions described in Section 2 are studied, confirming the observation from the $Z \rightarrow \mu\mu$ decays that the discrepancy between data and simulation is larger in the high $|\eta|$ regions.

In summary, when looking at the muon momentum resolution using the first pass reconstruction with preliminary calibration and alignment constants, the performance in data is worse than in simulation. The barrel region has been studied extensively using cosmics rays in the past [4, 3]: for both ID and MS, residual miscalibrations and misalignment in data reduce the agreement with the simulation. An additional discrepancy between data and simulation in the MS, coming from the term constant in p_T, is also observed and is being investigated. In the ID, for the end-caps, the use of preliminary alignment constants in this reconstruction pass introduces some disagreements with respect to expectations. For the MS, the alignment and calibration in the end-caps instrumented with MDT chambers are observed to be essentially similar to the barrel. For the CSC/no-TRT region the 2010 p-p collisions are the first data that allow the reconstruction performance for high-p_{T} tracks to be studied in detail. The limitations of the initial detector positioning used by the first pass reconstruction become visible as a discrepancy between the simulated and measured resolutions. This difference rises with p_{T}, as shown in Figure 3, and is attributed to the quality of the internal ID and MS alignment.

5.3 Input quantities to the combined fit

To measure the overall resolution and to determine the corrections needed for simulation we use the following inputs:

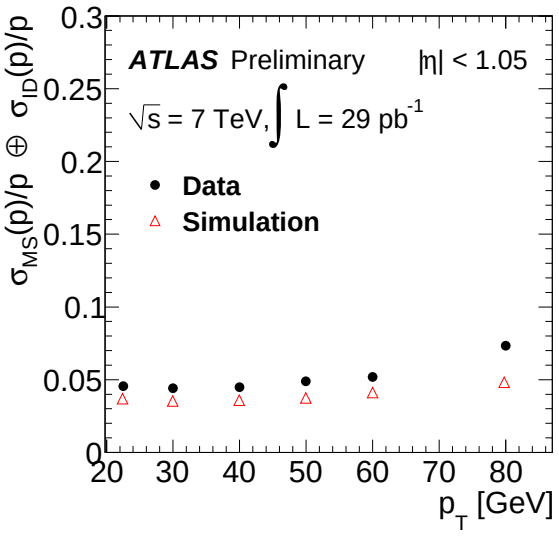

(a) Resolution p_{T} dependence for $0 < |\eta| < 1.05$

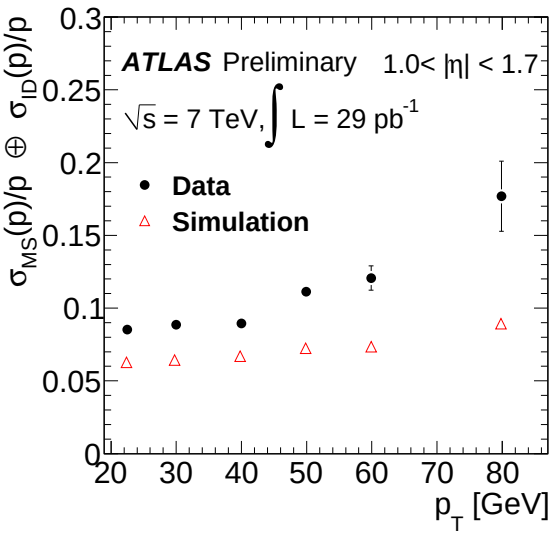

(b) Resolution p_{T} dependence for $1.05 < |\eta| < 1.7$

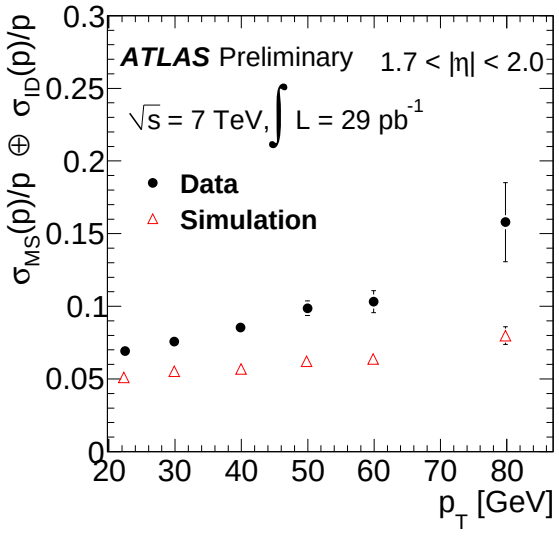

(c) Resolution p_{T} dependence for $1.7 < |\eta| < 2.0$

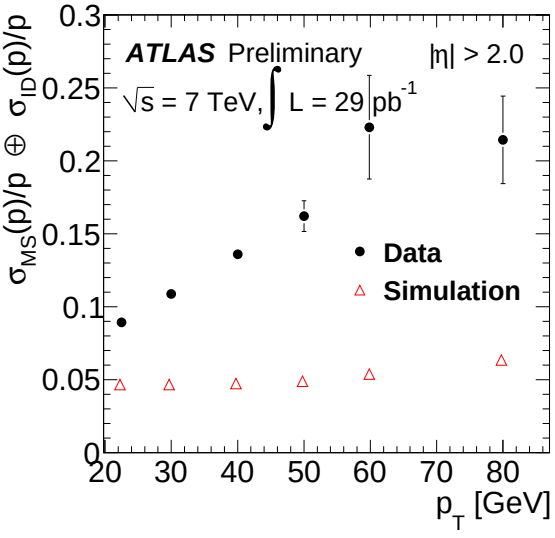

(d) Resolution p_{T} dependence for $2.0 < |\eta| < 2.5$

Figure 3: Sum in quadrature of the MS and ID resolutions as a function of muon p_{T}, for the four pseudorapidity regions. Data, selected according to the requirements in the text (dots) are compared with signal $W \rightarrow \mu\nu_{\mu}$ Pythia Monte Carlo simulation (open triangles) [6, 7]. This quantity accumulates the alignment and calibration effects from both tracking systems, therefore any discrepancy between data and simulation is expected to shrink when more detailed alignment and calibration corrections are made in subsequent analysis.

- The di-muon invariant mass in the Z boson mass region;
- The MS-to-ID curvature difference weighted by the muon electric charge, $(\frac{q}{p_{\mathrm{T}}^{ID}} - \frac{q}{p_{\mathrm{T}}^{MS}})$. The weighting by the electric charge disentangles systematic effects of the curvature due to local misalignments from the overall intrinsic resolution, reducing the bias on the estimation of the resolution and correction parameters.

For the simulation, we consider contributions from the Z and W boson decays into muons and the following background processes: Drell-Yan di-muon production, $t\bar{t}$, where one or two muons are generated, $Z \to \tau\tau$ and $W \to \tau\nu$; and heavy flavour decays ($b\bar{b}$, $c\bar{c}$) with one or two muons in the final state. Events and muons are selected as described in Section 4. In addition, it is required for data and simulation that the event be triggered by the level-1 muon trigger and a uniform p_{T} threshold of 10 GeV is applied to the muon candidate from the trigger chain in order to guarantee an unbiased determination of the correction parameters. For the $W \to \mu\nu_{\mu}$ events entering the combined fit the p_{T} cut is tightened to 25 GeV as a measure to improve the stability of the combined fit. The difference between reconstructed and true momentum resolution on simulation was examined and showed a Gaussian distribution with highly suppressed tails in the p_{T} and η ranges considered.

5.4 Combined fitting technique

The measurements of the MS and ID momentum resolution are obtained using a Monte Carlo template technique: a series of distributions of $\sigma(M)$ and ρ are created for various momentum resolution values and then matched to the one in data. For the MS the transformation is the following:

$$p'_{\mathrm{T}}(MS) = p_{\mathrm{T}}(MS) \;\; (1 + \Delta(MS)) \tag{7}$$

where

$$\Delta(MS) = f(0,1) \;\; \Delta p_1^{MS} + f(0,1) \;\; \Delta p_2^{MS} \;\; p_{\mathrm{T}} \tag{8}$$

$p'_{\mathrm{T}}(MS)$ indicates the simulated muon p_{T} after applying the corrections Δp_i^{MS}, while $f(0,1)$ is a normally distributed random number with mean 0 and width 1.

For the ID the rescaled p_{T} is expressed in the same way as :

$$p'_{\mathrm{T}}(ID) = p_{\mathrm{T}}(ID) \;\; (1 + \Delta(ID)) \tag{9}$$

where

$$\begin{aligned} \Delta(ID) &= f(0,1) \;\; \Delta p_2^{ID} \;\; p_{\mathrm{T}} \quad (|\eta| < 1.9) \\ \Delta(ID) &= f(0,1) \;\; \Delta p_2^{ID} \;\; p_{\mathrm{T}} / \tan^2(\theta) \quad (|\eta| > 1.9) \end{aligned} \tag{10}$$

$p'_{\mathrm{T}}(ID)$ indicates the simulated muon p_{T} after applying the corrections Δp_i^{ID} and θ is the muon polar angle. The values of the additional resolution $\Delta(ID), \Delta(MS)$ are obtained from a χ^2 minimisation fit to the overall spectrum (sum of all inputs for ID and MS and in the various $|\eta|$ regions). The variation of the $p_i^{ID,MS}$ parameters is performed by rescaling the simulated muon p_{T}.

An iterative smearing procedure is performed in which first we correct the p_{T} of single muons and pairs of muons from Z boson decays in the barrel region. Then the additional corrections are extracted for events in which one of the two muons or both fall in the $|\eta| > 1.05$ range.

5.5 External constraints to the combined fit

In the fitting procedure, additional knowledge is introduced from independent studies, both for the ID and the MS. This reduces the correlation among the multiple scattering and the detector resolution terms in the fit, resulting in smaller uncertainties on the fitted parameters. The way this external knowledge is translated into fit constraints is described in Section 5.6.

5.5.1 Multiple scattering in ID and MS

For the ID, the correction to the multiple scattering term in the ID, Δp_1^{ID}, is constrained around an expected value of zero, using the uncertainty on the ID material budget. The latter has been probed by the results on the K_s^0 reconstructed mass (sensitive to energy loss corrections) [15], the J/ψ width [16] and the resolution on the transverse impact parameter for low p_{T} ID tracks [17]. The material uncertainty from these studies is transformed in an approximation into 5% uncertainty on the multiple scattering correction term for $|\eta| < 2.0$, and 10% for $|\eta| > 2.0$.

For the MS, the multiple scattering term, Δp_1^{MS}, is a free parameter of the fit. The energy loss of muons is mainly concentrated in the calorimetry and has been measured in [9]. Its contribution to the overall MS resolution in the transverse momentum range from 20 to 100 GeV is negligible and therefore no additional contribution for the energy loss in the calorimetry, Δp_0^{MS}, is included.

5.5.2 MS alignment

In treating the corrections to the MS, where the Δp_1^{MS} and Δp_2^{MS} are highly correlated (up to 80% correlation) in the p_{T} region of interest, we apply our best estimate of the initial alignment accuracy. This is the result of commissioning studies from 2009 and 2010, on a large sample of cosmic ray events and samples of straight tracks obtained in periods of collision data taken with no magnetic field in the muon system. The estimated accuracy is shown in Table 1 for the various η regions. Such figures reflect results from different sources: for the MDT barrel region they come essentially from studies with cosmic ray muons [3] and are monitored with the relative optical alignment system; for the transition region and for the end-caps our current knowledge comes mainly from the optical system and is confirmed by a study with straight cosmic muon tracks, though statistically limited. About 10% of the chambers in the transition region are not monitored with alignment sensors. Their position is currently known at the level of about 1 mm. The position of the CSC chambers has been measured with straight muon tracks and found to agree within 700 μm with the positions used in track reconstruction.

This information can be translated directly into a constraint on the correction to the intrinsic resolution term in the MS, Δp_2^{MS}, by making use of the formula for the track sagitta:

$$\Delta s[\mu\mathrm{m}] \propto \frac{0.3}{8} B[\mathrm{T}]\, L[\mathrm{m}]^2\, \Delta p_2^{MS}[\mathrm{TeV}^{-1}]\, 10^3 \tag{11}$$

where Δs is the difference in sagitta from a correction Δp_2^{MS}, in a magnetic field of intensity B, given a track length L. The uncertainty on Δp_2^{MS} is propagated directly from the uncertainty on the alignment accuracy using the above formula. The resulting constraints on Δp_2^{MS} are summarized in Table 1. Since the statistical power of the measurement is not yet sufficient to probe the fraction of chambers in the

η region	Accuracy on alignment (μm)	Constraint on Δp_2^{MS} (TeV^{-1})
barrel	100 ± 20	0.20 ± 0.04
transition	100 ± 50	0.20 ± 0.07
end-caps	100 ± 50	0.20 ± 0.07
CSC/no TRT	700 ± 200	0.7 ± 0.2

Table 1: Alignment accuracy for the various regions of the MS corresponding to the 2010 first pass reconstruction. These values are obtained from the cosmic ray data and collision runs with no toroidal magnetic field ("straight track runs"). They are used to constrain the amount of correction needed on simulation to reproduce the MS intrinsic resolution term on data.

transition region whose alignment is determined with a less good accuracy (1 mm), we study the muon momentum resolution for that region as a whole. A systematic uncertainty on the measurement of the resolution in data is quoted to quantify this effect.

5.6 Combined fit results

The constraints on the Δp_i parameters from Section 5.5 are applied in the combined fit by adding a penalty term $\sum_i (\frac{\Delta p_i - a_i}{\sigma_{a_i}})^2$ to the total χ^2 being minimized. Here a_i is the expectation value and σ_{a_i} the associated uncertainty for each of the constrained Δp_i parameters. For the alignment accuracy in the MS they are the ones of Table 1. For the ID multiple scattering, the expected value a is set to 0. The value of σ_a is the needed absolute correction corresponding to a 5% (10%) relative deviation of p_1^{ID} from the Monte Carlo value for $|\eta| < 2.0$ ($|\eta| > 2.0$). The Δp_2^{ID} for the CSC/no-TRT region is obtained using the parameterization of Equation 3.

The fitted corrections parameters are provided in Table 2 together with their statistical and systematic uncertainties. The latter are discussed in the next section. For the Δp_2^{ID} parameter Equation 3 is used in the CSC/no-TRT region and Equation 2 for the other regions.

	MS		ID	
η region	Δp_1^{MS} (%)	Δp_2^{MS} (TeV^{-1})	Δp_1^{ID} (%)	Δp_2^{ID} (TeV^{-1})
barrel	$2.60 \pm 0.10 \pm 0.04$	$0.21 \pm 0.05 \pm 0.01$	0.03 ± 0.32	$0.396 \pm 0.044 \pm 0.008$
transition	$6.95 \pm 0.23 ^{+0.80}_{-0.00}$	$0.193 \pm 0.09 ^{+0.06}_{-0.15}$	$0.03 \pm 0.54 ^{+0.10}_{-0.00}$	$0.900 \pm 0.091 ^{+0.05}_{-0.00}$
end-caps	$3.45 \pm 0.35 \pm 0.05$	$0.21 \pm 0.12 \pm 0.01$	0.04 ± 0.58	$1.324 \pm 0.045 \pm 0.013$
CSC/no TRT	$4.05 \pm 0.61 \pm 0.22$	$0.90 \pm 0.19 \pm 0.16$	0.07 ± 0.50	$0.129 \pm 0.004 \pm 0.001$

Table 2: Set of corrections to be applied to the p_{T} parameterization of the simulated resolution in the MS and ID to reproduce the one in data. For example, in the MS barrel region the simulated multiple scattering term needs to be increased by an absolute 2.6% to match the one in data. The first uncertainty is statistical, the second one the quadratic sum of all systematic uncertainties. The statistical uncertainty is rescaled as explained in Section 5.7. The systematic uncertainties are discussed in Section 5.7 and their individual values are provided in Table 4.

The values of the correction parameters quantify the increase in momentum resolution in data when compared to simulation. The full parametrization of the experimental momentum resolution is obtained by adding quadratically the uncorrected simulated resolution terms of Equations 1–3 and the corresponding corrections from Table 2. The uncertainties are directly propagated from those of the correction parameters and the statistical errors on the uncorrected Monte Carlo resolution. The results for the full parametrization are listed in Table 3.

5.7 Systematic error sources

Given the uncertainty on the current knowledge of the material budget in the ID, the results of the resolution fit are tested by constraining the multiple scattering correction in the ID to the expected value and standard deviation as in Section 5.6. In the transition region some chambers in the MS are known to be less well aligned than others, therefore the effect of applying a uniform constraint to Δp_2^{MS} is also investigated.

The first effect (ID multiple scattering constraint) is evaluated by performing the fit for the Δp_1^{MS}, Δp_2^{MS} and Δp_2^{ID} parameters after fixing Δp_1^{ID} to the absolute value of Table 4, corresponding to a relative

η region	MS			ID	
	p_0^{MS} (TeV)	p_1^{MS} (%)	p_2^{MS} (GeV^{-1})	p_1^{ID} (%)	p_2^{ID} (TeV^{-1})
barrel	0.23 ± 0.01	3.75 ± 0.10	0.24 ± 0.04	1.60 ± 0.32	0.49 ± 0.04
transition	0	8.80 ± 0.46	0.30 ± 0.16	2.60 ± 0.54	0.95 ± 0.10
end-caps	0	4.77 ± 0.35	0.23 ± 0.12	3.40 ± 0.58	1.39 ± 0.05
CSC/no TRT	0.17 ± 0.02	4.87 ± 0.65	0.90 ± 0.25	4.10 ± 0.50	0.140 ± 0.004

Table 3: Resolution parametrization as defined in Equations 1–3 in the MS and ID. The measurements are obtained by adding the correction parameters in quadrature to the uncorrected momentum resolution from simulation.

5% (10%) σ. The systematic uncertainty on the other corrections is taken as the difference of each fitted value with respect to the baseline case.

The systematic uncertainty originated by imposing a single constraint to Δp_2^{MS} from the alignment accuracy in the transition region is also quantified. About 30% of the muons in the transition region have $1.05 < |\eta| < 1.2$, corresponding to the less well known part of the geometry. To assess the correctness of the $(100 \pm 50)\,\mu$m accuracy assumed for the whole region in the baseline analysis, all muons within the latter η range are removed and the fit is repeated. The additional systematic uncertainty for the transition region is shown in Table 4.

Finally, residual shape mismodeling in the simulation or incompatibilities with the constraints are accounted for by rescaling the statistical uncertainty σ_{stat} returned by the baseline fit. Both effects would produce a $\chi^2/N_{\text{d.o.f.}}$ (with $N_{\text{d.o.f.}}$ the overall number of degrees of freedom) different from 1: therefore we use as statistical uncertainty the quantity $\sigma'_{\text{stat}} = \sigma_{\text{stat}}\sqrt{\chi^2/N_{\text{d.o.f.}}}$ [14]. Values of $\chi^2/N_{\text{d.o.f.}}$ between 1.1 and 1.5 are used, depending on the η region.

In this context, an additional check of the goodness of the constraints from the external alignment accuracy is performed. This is not considered in the evaluation of the systematic uncertainties, but rather as an independent control. The gaussian constraint of Section 5.6 is completely removed and Δp_2^{MS} is let to vary freely in the fit. A χ^2 minimization for the unconstrained Δp_2^{MS} is performed. The Δp_2^{MS} corresponding to the minimum χ^2 and the bounds of the 2σ interval are the following:

- Barrel: $\Delta p_2^{MS}(\chi^2_{\text{min}})$ = 0.25 TeV^{-1}; 2σ interval = [0.05, 0.40]
- Transition: $\Delta p_2^{MS}(\chi^2_{\text{min}})$ = 0.25 TeV^{-1}; 2σ interval = [0.0, 0.3]
- End-caps: $\Delta p_2^{MS}(\chi^2_{\text{min}})$ = 0.0 TeV^{-1}; 2σ interval = [0.0, 0.3]
- CSC/no TRT: $\Delta p_2^{MS}(\chi^2_{\text{min}})$ = 0.2 TeV^{-1}; 2σ interval = [0.0, 0.4]

The test proves the fit consistency with the external alignment constraints imposed; furthermore it shows the sensitivity of a fully free fit to the Δp_2^{MS} parameter in the p_{T} range probed with the available data sample.

5.8 Measured resolutions as a function of p_{T}

The parametrized resolution as a function of p_{T} for the four η regions, obtained using the values of the parameters from the combined fits, are shown separately in Figures 4 and 5 for the MS and the ID, respectively. The resolution curves for experimental data are compared to those from the uncorrected parameters obtained for the simulation. The results of the analysis on collision data is also compared with the resolution curves obtained from analysis of cosmic ray muons [3]. Results using comic rays

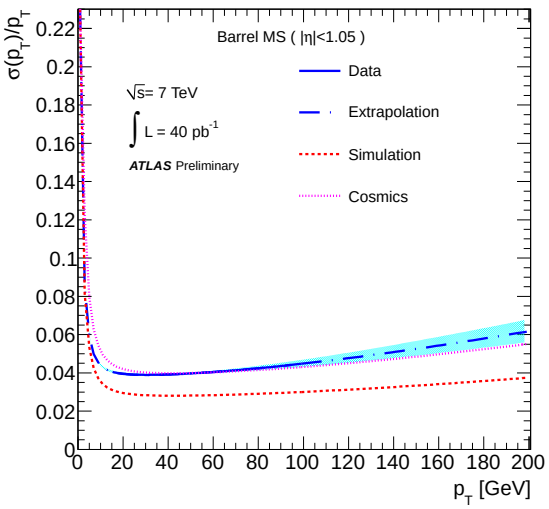

(a) MS resolution p_{T} curve for $0 < |\eta| < 1.05$

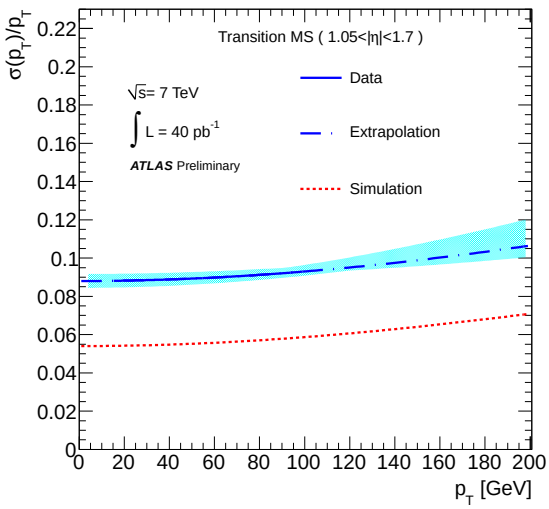

(b) MS resolution p_{T} curve for $1.05 < |\eta| < 1.7$

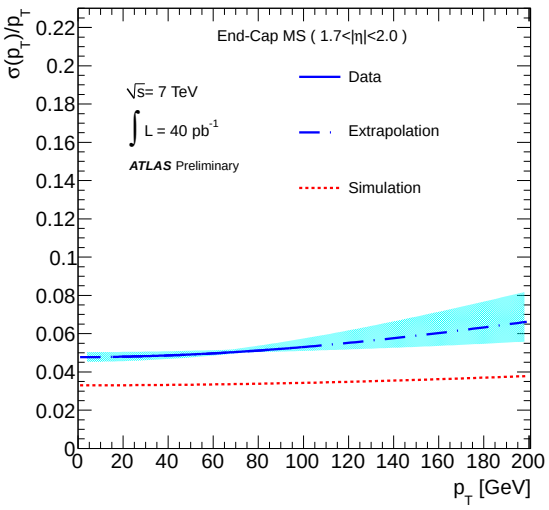

(c) MS resolution p_{T} curve for $1.7 < |\eta| < 2.0$

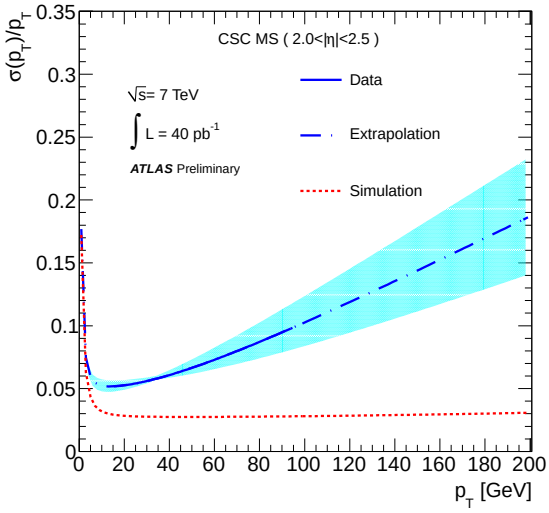

(d) MS resolution p_{T} curve for $2.0 < |\eta| < 2.5$

Figure 4: Resolution curve from the fitted parameter values of the MS in collision data and simulation as a function of the muon p_{T}, for the different η regions of the detector. The solid blue line shows determinations based on data and is continued as dashed line for the extrapolation to p_{T} ranges not accessible in this analysis. The shaded band represents the sum in quadrature of the statistical and systematic uncertainties. For the case of the barrel, a comparison with the curve obtained from the fitted parameters from cosmic ray data is overlaid for comparison.

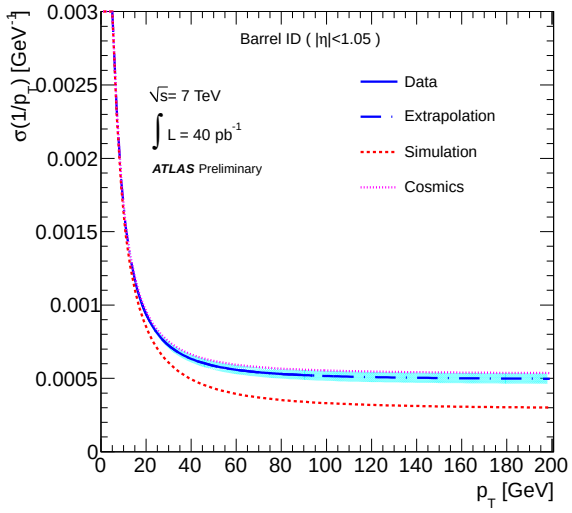

(a) ID resolution p_{T} curve for $0 < |\eta| < 1.05$

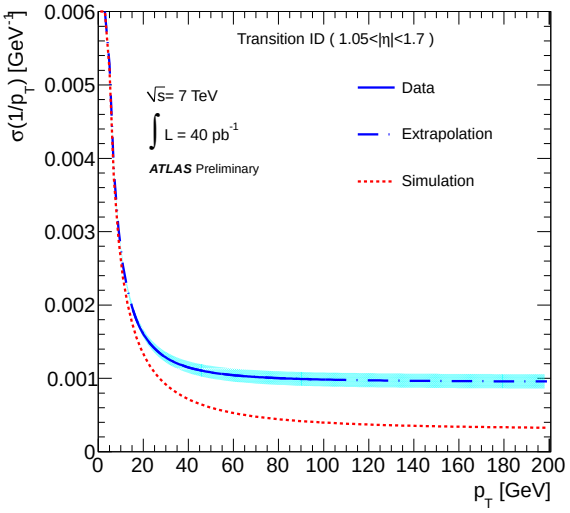

(b) ID resolution p_{T} curve for $1.05 < |\eta| < 1.7$

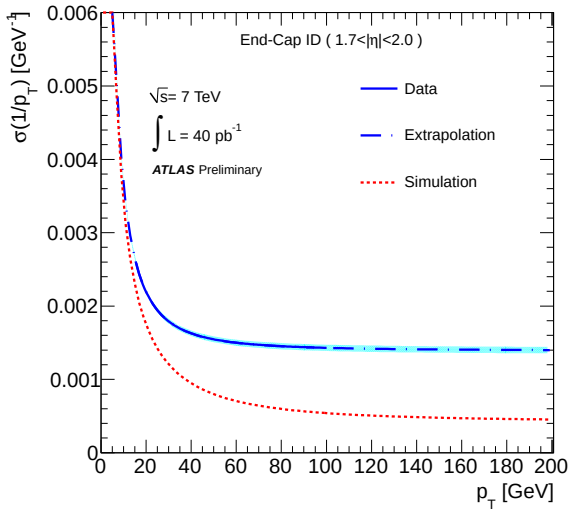

(c) ID resolution p_{T} curve for $1.7 < |\eta| < 2.0$

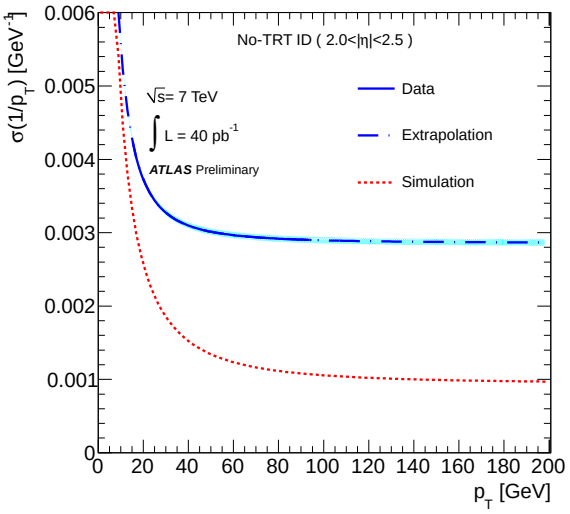

(d) ID resolution p_{T} curve for $2.0 < |\eta| < 2.5$

Figure 5: Resolution curve on the curvature, $\sigma(1/p_{\mathrm{T}})$, from the fitted parameter values of the ID in collision data and simulation as a function of the muon p_{T} for the different $|\eta|$ regions. The solid blue line shows measurements on data and is continued as dashed line for the extrapolation to p_{T} ranges not accessible in this analysis. The shaded band represents the sum in quadrature of the statistical and systematic uncertainties.

Source	η region	MS		ID	
		Δp_1^{MS} (%)	Δp_2^{MS} (TeV^{-1})	Δp_1^{ID} (%)	Δp_2^{ID} (TeV^{-1})
ID mult. scattering	barrel	± 0.041	± 0.006	0.51 (*fixed*)	± 0.008
	transition	± 0.00	± 0.057	0.83 (*fixed*)	± 0.000
	end-caps	± 0.05	± 0.009	1.09 (*fixed*)	± 0.013
	CSC/no TRT	± 0.22	± 0.16	2.20 (*fixed*)	± 0.0002
MS alignment ($1.05 < \|\eta\| < 1.2$)	transition	$+0.8$	-0.14	$+0.1$	$+0.05$

Table 4: Systematic uncertainty on the correction parameters, divided by source. Δp_1^{ID} indicated as *fixed* are set to the value in the table, corresponding to the Monte Carlo value of Δp_1^{ID} + 1σ, following the procedure described in Section 5.7.

are only available for the MS barrel region and show a good agreement with the presented results for p_{T} larger than 20 GeV. At lower transverse momenta the cosmic ray results are biased by the fluctuations in the muon energy loss. The associated systematic uncertainty is of the same order as the disagreement between the cosmic ray and the collision results in Figure 4.

5.9 Correction formula for combined muons

The combined muon momentum measurement is determined by the relative weights of the ID and MS momentum measurements in the track fit. Due to the large amount of calorimeter material between ID and MS, the two measurements can be treated as uncorrelated. Therefore, starting from the corrected ID and MS p_{T} measurements in Monte Carlo, we can correct the combined muon $p_{\mathrm{T}}(CB)$ in the simulation and obtain a new measurement, $p'_{\mathrm{T}}(CB)$. The new Monte Carlo measurement is the linear combination of the MS and ID contributions, weighted by the MS and ID resolutions:

$$p'_{\mathrm{T}}(CB) = p_{\mathrm{T}}(CB)\ [1 + \frac{\frac{\Delta(MS)}{\sigma^2(MS)} + \frac{\Delta(ID)}{\sigma^2(ID)}}{\frac{1}{\sigma^2(MS)} + \frac{1}{\sigma^2(ID)}}] \tag{12}$$

where $\Delta(MS,ID)$ is the overall correction to the simulated MS or ID p_{T}, from Equations 7 and 9; and $\sigma(MS,ID)$ are the values for the resolution at that $p_{\mathrm{T}}(MS,ID)$, taken from Table 3.

The results of the correction of the Monte Carlo simulation for the MS, ID and combined momentum measurement, compared with data for the di-muon invariant mass in the Z region are shown in the Appendix.

6 Conclusions

A determination of the muon momentum resolution is presented for the full integrated luminosity of 40 pb^{-1} p-p collision data collected in 2010 with the ATLAS detector. Different physics channels have been used to evaluate the resolution as a function of the muon p_T and η, for both the muon spectrometer and the inner detector. Combining all the information, the momentum scale and resolution were measured on the experimental data and compared to simulation. A correction function is presented which allows the muon momentum resolution in simulation to model closely the one in data over a wide range of momenta.

The results show that the expected resolution on simulation is not yet fully achieved with the use of preliminary alignment and calibration constants in the first-pass reconstruction. Subsequent analysis of the muon momentum resolution indicates that the resolution is improved when more detailed alignment and calibration corrections are made.

References

[1] ATLAS Collaboration, *The ATLAS Experiment at the CERN Large Hadron Collider*, JINST **3** (2008) S08003.

[2] ATLAS Collaboration, *Determination of the muon reconstruction efficiency in ATLAS at the Z resonance in p-p collisions at* $\sqrt{s} = 7$ *TeV*, ATLAS-CONF-2011-008 (2011) .

[3] ATLAS Collaboration, *Commissioning of the ATLAS Muon Spectrometer with Cosmic Rays*, Eur. Phys. J. **C 70** (2010) 875.

[4] ATLAS Collaboration, *The ATLAS Inner Detector commissioning and calibration*, Eur. Phys. J. **C 70** (2010) 787.

[5] ATLAS Collaboration, *Performance of the ATLAS Muon Trigger in p-p collisions at* $\sqrt{s}$ *= 7 TeV*, ATLAS-CONF-2010-095 (2010) .

[6] T. Sjöstrand, S. Mrenna, and P. Skands, *PYTHIA 6.4 Physics and Manual*, JHEP **05** (2006) 026.

[7] ATLAS Collaboration, *The ATLAS Simulation Infrastructure*, Eur. Phys. J. **C 70** (2010) 823.

[8] GEANT-4 Collaboration, S. Agostinelli et al., *Geant4: A simulation toolkit*, Nucl. Instrum. Meth. **A506** (2003) .

[9] ATLAS Collaboration, *Studies of the performance of the ATLAS detector using cosmic-ray muons*, acc. by Eur. Phys. J. (2011) , `arXiv:1011.6665 [physics.ins-det]`.

[10] ATLAS Collaboration, *Measurement of the* $W \to \ell\nu$ *and* $Z/\gamma^* \to \ell\ell$ *production cross sections in proton-proton collisions at* $\sqrt{s} = 7$ *TeV with the ATLAS detector*, JHEP **12** (2010) 060.

[11] R. K. Ellis, W. J. Stirling, and B. R. Webber, *QCD and Collider Physics*. Cambridge University Press, Cambridge, UK, 1996.

[12] ATLAS Collaboration, *Alignment Performance of the ATLAS Inner Detector Tracking System in 7 TeV proton-proton collisions at the LHC*, ATLAS-CONF-2010-067 (2010) .

[13] ATLAS Collaboration, *Alignment of the ATLAS Inner Detector Tracking System with 2010 LHC proton-proton collisions at sqrt(s) = 7 TeV*, ATLAS-CONF-2011-012 (2011) .

[14] Particle Data Group Collaboration, K. Nakamura et al., *Review of Particle Properties*, J. Phys. G **37** (2010) 075021.

[15] ATLAS Collaboration, *Study of the Material Budget in the ATLAS Inner Detector with* K^0_s *decays in collision data at sqrt(s)=900 GeV*, ATLAS-CONF-2010-019 (2010) .

[16] ATLAS Collaboration, J/ψ *Performance of the ATLAS Inner Detector*, ATLAS-CONF-2010-078 (2010) .

[17] ATLAS Collaboration, *Tracking Studies for b-tagging with 7 TeV Collision Data with the ATLAS Detector*, ATLAS-CONF-2010-070 (2010) .

Appendix

Validation of the simulation smearing

To indicate the goodness of the simulation corrections provided in Section 5, Figure 6 shows the distribution of the di-muon invariant mass in the Z region after applying the corrections. The comparison displays good agreement between data and Monte Carlo simulation.

In perspective: first results with reprocessed data

In this note the muon resolution was measured in the 2010 data processed with the first-pass ATLAS reconstruction, using the preliminary calibration and alignment constants for both ID and MS detectors. The reprocessing of the whole 2010 dataset completed lately indicates that, making use of more refined knowledge of the alignment, calibration and magnetic field layout, a better performance and a more satisfying agreement with expectations is achieved. To illustrate the subsequent improvements, Figure 7 shows the reconstructed di-muon invariant mass around the Z pole, comparing combined muon tracks in first-pass reconstruction and reprocessing. The better agreement between data and simulation is mainly the result of the improved alignment. Further improvements are expected for the 2011 data taking due to additional refinements of the detector calibration and alignment.

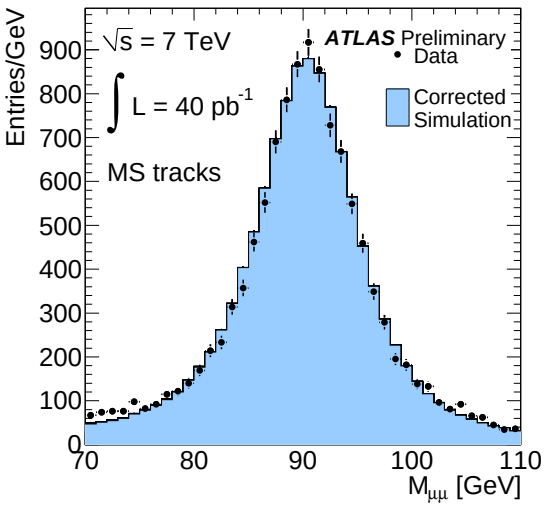

(a) Di-muon invariant mass after correction, MS

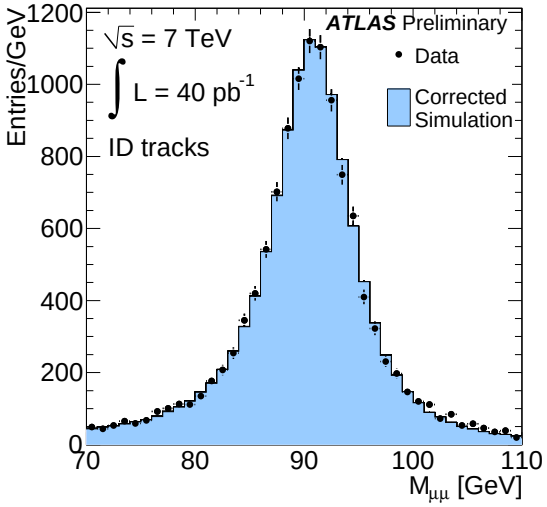

(b) Di-muon invariant mass after correction, ID

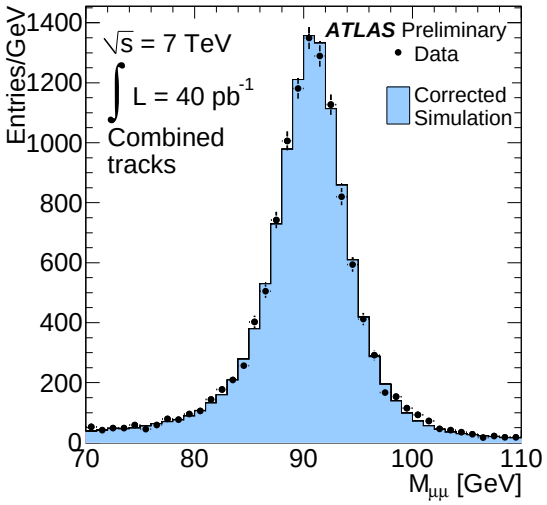

(c) Di-muon invariant mass after correction for combined muons

Figure 6: Di-muon invariant mass comparison in the Z boson mass range between collision data (dots) and simulation (full histogram), after correcting the simulated muon p_{T} by the parameters derived in this study. The distributions are integrated over the full range of η. From top left to bottom: MS, ID and combined measurements are shown.

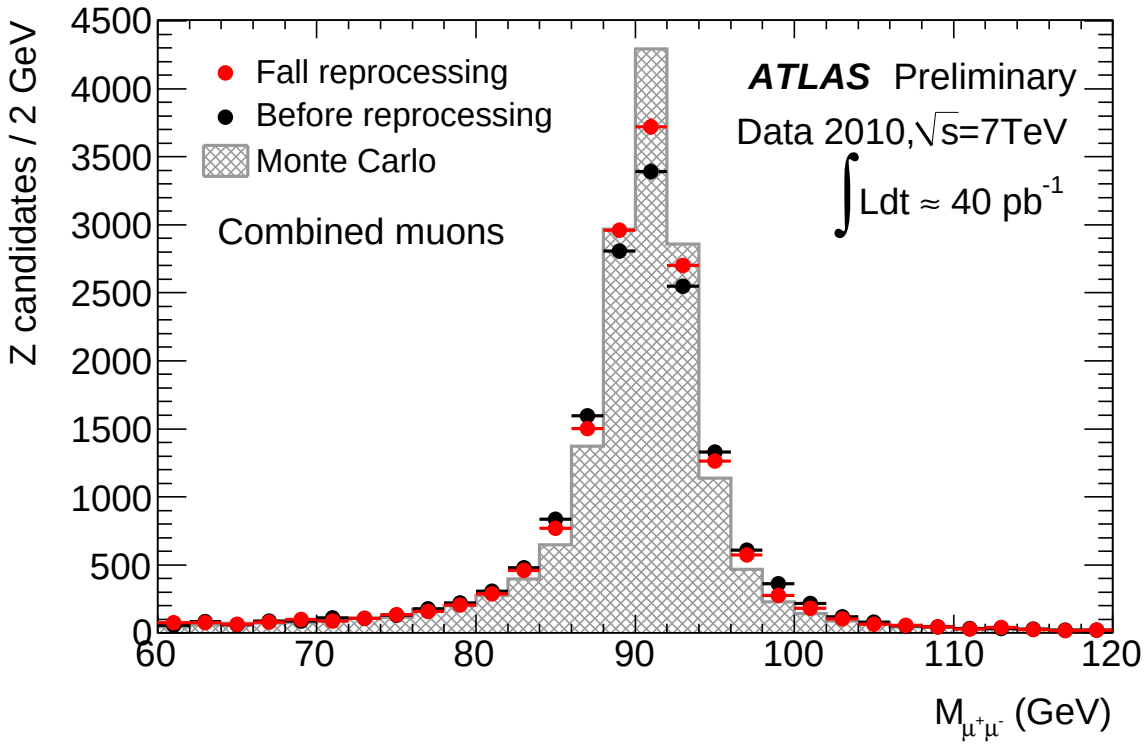

Figure 7: Di-muon invariant mass in the Z boson mass region, for data processed with the prompt reconstructions (black dots), the Fall 2010 reprocessing (red dots) and simulation (grey full histogram). Combined measurements are shown. The integrated luminosity corresponds to $40\,\mathrm{pb}^{-1}$.